https://doi.org/10.1093/nar/gkac886

A PAM-free CRISPR/Cas12a ultra-specific activation mode based on toehold-mediated strand displacement and branch migration

You Wu[1,†], Wang Luo[1,†], Zhi Weng[1], Yongcan Guo[2], Hongyan Yu[1], Rong Zhao[1], Li Zhang[1], Jie Zhao[3], Dan Bai[1], Xi Zhou[1], Lin Song[1], Kena Chen[1], Junjie Li[1,*], Yujun Yang[1,*] and Guoming Xie[1,*]

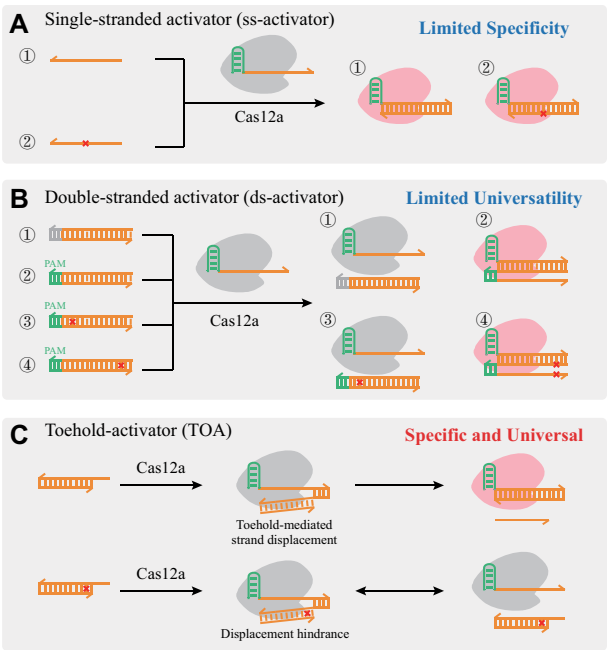
[1]Key Laboratory of Clinical Laboratory Diagnostics (Chinese Ministry of Education), College of Laboratory Medicine, Chongqing Medical Laboratory Microfluidics and SPRi Engineering Research Center, Chongqing Medical University, Chongqing, 400016, PR China, [2]Clinical Laboratory of Traditional Chinese Medicine Hospital Affiliated to Southwest Medical University, Luzhou, 646000, PR China and [3]Clinical Molecular Medicine Testing Center, The First Hospital of Chongqing Medical University, No. 1 Youyi Road, Yuzhong District, Chongqing, 400016, PR China

Received July 05, 2022; Revised September 26, 2022; Editorial Decision September 27, 2022; Accepted October 28, 2022

ABSTRACT

CRISPR (clustered regularly interspaced short palindromic repeats) technology has achieved great breakthroughs in terms of convenience and sensitivity; it is becoming the most promising molecular tool. However, only two CRISPR activation modes (single and double stranded) are available, and they have specificity and universality bottlenecks that limit the application of CRISPR technology in high-precision molecular recognition. Herein, we proposed a novel CRISPR/Cas12a unrestricted activation mode to greatly improve its performance. The new mode totally eliminates the need for a protospacer adjacent motif and accurately activates Cas12a through toehold-mediated strand displacement and branch migration, which is highly universal and ultra-specific. With this mode, we discriminated all mismatch types and detected the EGFR T790M and L858R mutations in very low abundance. Taken together, our activation mode is deeply incorporated with DNA nanotechnology and extensively broadens the application boundaries of CRISPR technology in biomedical and molecular reaction networks.

GRAPHICAL ABSTRACT



INTRODUCTION

The clustered regularly interspaced short palindromic repeats (CRISPR) system can quickly target specific gene sequences (activators) by CRISPR RNA (crRNA) and activate the cleavage activity of Cas nuclease. Due to high programmability and reactivity, CRISPR has been widely

*To whom correspondence should be addressed. Tel: +86 23 68485240; Fax: +86 23 68485239; Email: guomingxie@cqmu.edu.cn
Correspondence may also be addressed to Yujun Yang. Email: yangyujun@cqmu.edu.cn
Correspondence may also be addressed to Junjie Li. Email: lijunjie2006@gmail.com; jjayli2006@cqmu.edu.cn
†The authors wish it to be known that, in their opinion, the first two authors should be regarded as Joint First Authors.

© The Author(s) 2022. Published by Oxford University Press on behalf of Nucleic Acids Research.
This is an Open Access article distributed under the terms of the Creative Commons Attribution-NonCommercial License (http://creativecommons.org/licenses/by-nc/4.0/), which permits non-commercial re-use, distribution, and reproduction in any medium, provided the original work is properly cited. For commercial re-use, please contact journals.permissions@oup.com

Downloaded from https://academic.oup.com/nar/advance-article/doi/10.1093/nar/gkac886/6786210 by Shanghai Normal University user on 03 November 2022

applied in gene editing, intracellular imaging, transcriptional regulation, etc. (1). In addition, Class 2V and VI Cas nucleases, including Cas12a, Cas12b, Cas13a and Cas14a, have trans-cleavage activity for massively cleaved probes modified with a fluorophore and quencher (reporter) (2–4). These properties make Cas nucleases powerful nucleic acid recognizers and signal amplifiers.

CRISPR-based detection platforms have continuously emerged, which have made great breakthroughs in sensitivity and convenience (5–9) and realized detection of a variety of biomarkers such as viruses, bacteria, microRNA, etc. (2,7,10). However, there are only two available CRISPR activation modes based on single-stranded or double-stranded activators (ss- and ds-activators, respectively), which have technical bottlenecks in terms of specificity or universality. This has limited the application of CRISPR technology in high-precision molecular recognition, such as point mutation detection. DNA point mutations are key drivers of tumor development and important biomarkers of diagnosis and prognosis (11–13). Because of low abundance, various mutation types and small thermodynamic changes, most of them are difficult to detect (13,14). Therefore, developing a novel unrestricted CRISPR activation mode is quite promising. It will not only broaden the application of CRISPR technology in the biomedical field, but will also show great potential in high-precision molecular sensing, biochemical circuits and DNA reaction networks.

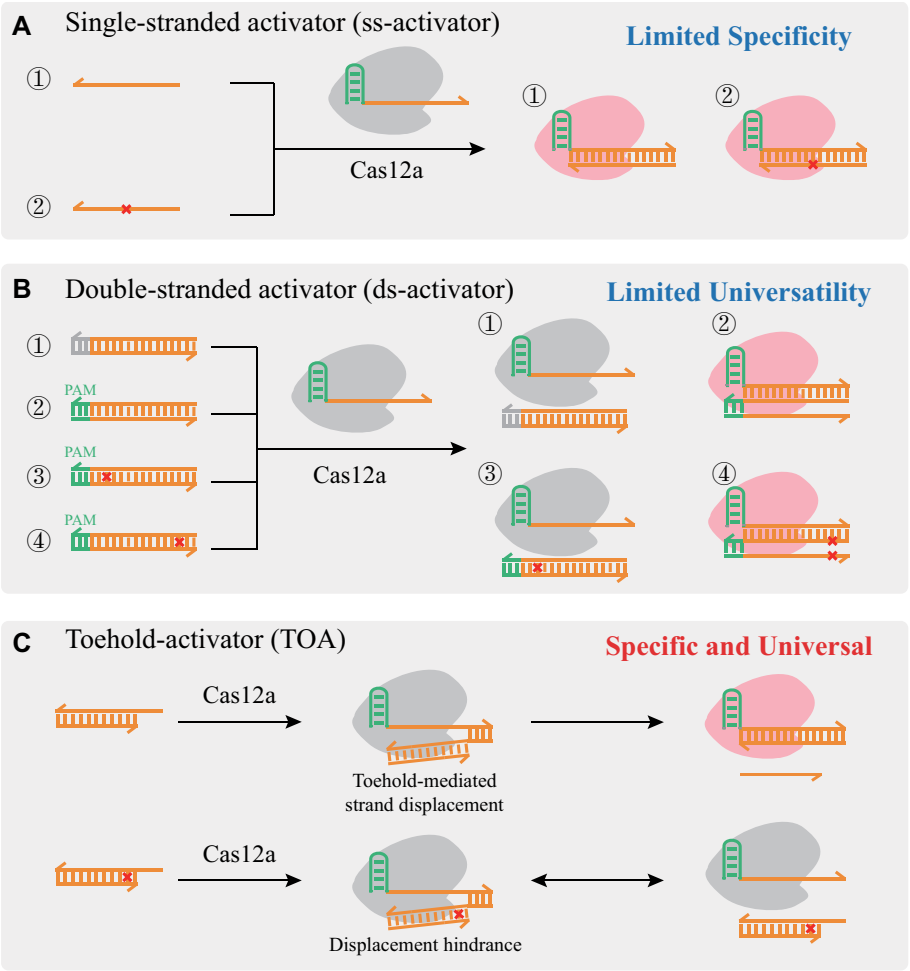
Using the T7 transcription process, the SHERLOCK platform generated ss-activators to activate Cas13a to detect subtypes of the Zika virus and dengue fragments (7). Through primer extension to displace the ss-activators, the AIOD-CRISPR platform activated Cas12a and realized the sensitive detection of severe acute respiratory virus coronavirus 2 (SARS-CoV-2) (15). These methods utilize ss-oligonucleotides as activators, because they are flexible to be produced or released. However, studies have demonstrated that single-base mismatch in ss-activators hardly hinders the activation of Cas nuclease (6). Thus, the ss-activation mode has a limited specificity (Scheme 1A). Furthermore, faulty ss-amplicons generated by out of control amplification may activate Cas to result in false positives (Supplementary Scheme S1A). Thus, its stability is also limited. In addition to ss-activators, Cas12 can be activated by dsDNA with a protospacer adjacent motif (PAM). Ds-activators are more stable, and Cas is not activated when mutations occur in or near their PAM (16,17). For example, The CDetection platform targeting dsDNA achieved simple and rapid mutation detection (18). However, PAMs near mutations are uncommon in the human genome (only 20 000 point mutations contain a PAM sequence out of 600 000 point mutations in the National Center for Biotechnology Information ClinVar database) (14). Therefore, the ds-activation mode has a very limited universality (Scheme 1B). Several researchers have attempted to insert a PAM near the mutation sites, while the range of effective insertion was extremely narrow (the accuracy decreases dramatically when a point mutation is >6 bases away from the PAM) (5,19–22). Balancing PAM amplification efficiency and mutation detection selectivity is difficult (Supplementary Scheme S1B), resulting in limited flexibility.

Toehold-mediated strand displacement reaction (TSDR) follows precise base-pairing rules and has great advantages in the recognition of single-base mismatches (23). In this reaction, the invasion strand binds to the short complementary ss-domain (toehold) on the ds-substrate, triggers the subsequent branch migration and eventually replaces the protector of the substrate to be the thermodynamically most stable state (24). When a single-base mismatch exists, the rate of strand displacement is dramatically decreased, and mutant-type targets can be discriminated from the wild type by kinetic difference (24). Herein, we firstly proposed the dsDNA containing a toehold as an activator to specifically activate CRISPR–Cas12a, which is called the toehold-activator (TOA). The toehold of the activator binds to the crRNA, and a DNA–crRNA complex is formed subsequently through strict TSDR. Eventually, the Cas nuclease is accurately activated. Based on the feature of TSDR, a single-base mismatch in the TOA will significantly reduce the DNA–crRNA complex formation and therefore decrease the activation efficiency. The signal generated by the cleaved reporter can amplify the activation efficiency difference and contribute to specifically distinguishing mutant targets. Moreover, different from the PAM, the position and orientation of the toehold can be flexibly adjusted, and arbitrary dsDNA can have a toehold by a simple process. Thus, the TOA may be far more specific and stable than the ss-activator, and more universal and flexible than the ds-activator (Scheme 1C).

The release of pre-blocked activators through the displacement of the invasion or fuel strands can improve the selectivity of the CRISPR system. However, the sequences of these displacement strands should largely overlap with that of activators (usually >60%) to release them rapidly. Given the non-specific feature of the ss-activation mode, such displacement strands will easily result in signal leakage (Supplementary Scheme S1C). Researchers had to tediously tune the number of overlapping bases to balance the velocity of activator release and signal leakage (25–27). Notably, this problem no longer exists in this work. Instead of the whole activator, we only needed to block and release several bases of the TOA's toehold to achieve a remarkable effect, which is almost impossible to result in unexpected activation. The branch migration (BM) reaction is a reversible reaction without base pair changes. When a mismatch occurs, the reaction balance is broken and the yield decreases dramatically. It has high specificity and can detect difficult mismatches with very low Gibbs free energy change (ΔG) in the GC-rich region (28). The structure of the BM probe (BMP) is very similar to that of the toehold-blocked TOA, and its working principle is compatible with TSDR. Therefore, we can selectively release the blocked toehold of TOA through BM reactions. Their cascade has the potential to achieve superior single-base specificity, and avoid the cumbersome overlapping in base adjustment to reduce the risk of signal leakage.

Considering the deficiency of ds- and ss-activation modes, for the first time, we present a novel CRISPR/Cas12a unrestricted activation mode to greatly improve the performance of CRISPR technology and expand its application boundaries. The activator binds crRNA by strict TSDR, is considerably more specific than

Downloaded from https://academic.oup.com/nar/advance-article/doi/10.1093/nar/gkac886/6786210 by Shanghai Normal University user on 03 November 2022



Scheme 1. Characteristics of different activation modes. Cas12a in gray represents inactivated, pink represent activated. The red '×' represents single-base mismatches in activators. (**A**) ss-activators activate Cas12a regardless of whether a single-base mismatch occurs. (**B**) Only the ds-activators containing a PAM can activate Cas12a, and they show discernment only when single-base mismatches occur in the vicinity of a PAM. (**C**) TOA specifically activates Cas12a by strict TSDR without a PAM.

ss-activators and can precisely detect any target sequence without a PAM, which is more universal than ds-activators. Cascading with the BM reaction, the new activation mode has remarkably improved the detection accuracy of CRISPR technology. The discrimination factors (DFs) of all types of single-base mismatches are satisfactory. Moreover, we developed an improved polymerase chain reaction (PCR) to obtain the ds-targets with ss-domains as the toehold-blocked TOA. Finally, we validated the potential of this method for practical application by detecting EGFR T790M and L858R mutations in low abundance.

MATERIALS AND METHODS

Materials

EnGen®Lba Cas12a (Cpf1, 100 μM, 20 μM) and CutSmart buffer [50 mM potassium acetate, 20 mM Tris-acetate, 10 mM magnesium acetate, 100 μg/ml bovine serum albumin (BSA), pH 7.9)] were ordered from New England Biolabs and MAGIGEN. The TranscriptAid T7 High Yield Transcription Kit and the RNeasy MinElute Cleanup Kit were obtained from ThermoFisher Scientific and Qiagen, respectively. Deoxynucleotide triphosphates (dNTPs), SYBR Green, diethylpyrocarbonate (DEPC)-treated water, eight strip real-time PCR tubes and caps, magnesium chloride, reporter, DNA sequences, uracil-DNA glycosylase (UDG) and PCR mix were purchased from Sangon Biotech Inc. (Shanghai, China) and Tsingke Biotechnology Co., Ltd (Beijing, China). The crRNAs used were synthesized with the TranscriptAid T7 High Yield Transcription Kit or obtained from Beijing Genomics Institution (Beijing, China). The nucleic acid extraction and purification kit was purchased from Burning Rock Biotech Ltd. (Guangzhou, China). *N*,*N*,*N*',N'-Tetramethylethylenediamine (TEMED) and 30% acrylamide/bis solution were provided by Sigma-Aldrich (St. Louis, MO, USA). DNA loading buffer (6×) and Gel Red nucleic acid dye were ordered from TaKaRa Biotech (Dalian, China). All chemical reagents were of analytical grade, and RNase-free water was used throughout this study.

Downloaded from https://academic.oup.com/nar/advance-article/doi/10.1093/nar/gkac886/6786210 by Shanghai Normal University user on 03 November 2022

Instrument

The endpoint fluorescence used to calculate the DF was detected by a Cary Eclipse Fluorescence spectrophotometer (Agilent, USA) (excitation wavelength = 535 nm, emission wavelength = 556 nm and both slits were 5 nm). The real-time fluorescence curves and endpoint fluorescence were detected by a Rotor-Gene 6000 instrument (Corbett Research, Mortlake, Australia). Gel images were obtained on an electrophoresis apparatus (DYY-6C, LIUYI, China) and imaging system (Bio-Rad Laboratories, USA). Fluorescent PCR signals were recorded by a real-time PCR instrument (CFX96, Bio-Rad, USA). The digital PCR (dPCR) was performed on a DQ24 dPCR instrument (Sniper Medical Technology Co., Ltd, China). The droplet volume can be controlled stably at 0.5–2 nl; min/max flow rate, 500–2000 nl/s; scanning frequency, 100–200 Hz; droplet generation method; vibration injection method; reaction volume, 20 μl; detection time, ∼1.5 h; temperature control range, 4–98°C; temperature control accuracy, ± 0.1°C. DNA concentration, purity and integrity were assessed by Nanodrop and Qubit 3.0 (Thermo Fisher, USA).

Methods

CRISPR/Cas12a reaction system. Cas12a–crRNA complexes were pre-assembled by incubating 2 μM LbCas12a with 2.4 μM crRNA at 37°C for 30 min. The complexes were diluted to a final concentration of 20 nM in a solution containing 1× Cutsmart Buffer, adding 250 nM ssDNA reporter substrates, and the final system is 20 μl.

TOA activation assays. TOA, ss-activator or ds-activator (40 nM) was added to the reaction system, reacted for 20 min at room temperature, and endpoint fluorescence was detected.

BM-TOA system for ss-target assays. BM probe and ss-target (20 nM) were added to the reaction system, reacted at 30°C and real-time and endpoint fluorescence was detected.

BM-TOA system for BMP-like target assays. BMP-like target and trigger (20 nM) were added to the reaction system, reacted at 30°C and real-time and endpoint fluorescence was detected.

Low-abundance L858R and T790M mutation assays. BMP-like target (200 nM) and trigger (400 nM) were added to the reaction system, reacted at 30°C and real-time and endpoint fluorescence was detected.

Post U-PCR assays. A 10 μl aliquot of Taq PCR Master Mix (2×), 0.5 μl of U-forward primer (10 μM), 1 μl of reverse primer (10 μM), 1 μl of synthetic template or DNA extraction solution of tumor tissues and 7.5 μl of ddH_2O were mixed in the PCR tube (an additional 1 μl of 20× SYBR for the melt curve). The PCR procedure (95°C for 10 s, 60°C for 15 s and 72°C for 15 s, 34 cycles) was performed on a Bio-Rad instrument. After amplification, 0.5 μl of UDG (2 U/μl) was used to digest the U-bases at 50°C for 5 min, and was inactivated at 90°C for 10 min. The product and 500 nM trigger were added to the reaction system, reacted at 30°C and real-time fluorescence was detected.

Digital PCR assays. A 12.5 μl aliquot of 2× dPCR Master Mix (Sniper), 1 μl of dPCR forward primer and dPCR reverse primer, 0.5 μl of MGB Probe (WT), 0.5 μl of MGB Probe (MT), 10 ng of extracted DNA of tumor tissues and ddH_2O to 20 μl were used. Procedure: 5 min of constant temperature at 60°C, 15 min of hot start at 98°C, one cycle; 10 s of denaturation at 95°C, 15 s of annealing at 60°C, 15 s of extension at 72°C, 40 cycles; 1 min of constant temperature at 50°C. The amplicon size is 172 bp. dPCR was performed on a DQ24 dPCR instrument, and the dPCR analysis program is SightPro v0.3.5. The individual partition volume was 0.8 nl, and the total volume of the partitions measured was 20 μl.

Patients and sample collection

The DNA clinical samples of the L858R mutation were extracted from tumor tissues (paraffin-embedded tissue specimens) of patients with non-small cell lung cancer (invasive lung adenocarcinoma) using the nucleic acid extraction and purification kit. These patients ($n = 11$) were enrolled in this study between June 2021 and April 2022 in the First Hospital of Chongqing Medical University. Tumor tissue was obtained from surgical resection or open biopsy for 11 patients in the study. These samples were formalin-fixed and processed into paraffin-embedded samples and were sectioned and then HE stained to assess whether tumor cells made up >20%. The tumor area of the tissue was scraped, dewaxed and DNA was extracted. The DNA extraction solutions from tumor tissues were assessed for concentration, purity and integrity by Nanodrop and Qubit 3.0 (>4 g/μl, N/Q <3.5). Samples were then stored at –80°C until assay. This research was approved by the Ethics Committee of Chongqing Medical University (Chongqing, China). All methods were carried out in accordance with the approved guidelines. Written informed consent was obtained from all patients.

Design and calculation

The sequence designs (Supplementary Table S1; Supplementary Schemes S2–S12) were supported by NUPACK, SnapGene and Oligo7. The thermodynamic parameters were calculated by NUPACK. The relationship between the toehold length and the reaction yield was calculated using MATLAB. The relationship of Gibbs free energy and the reaction yield is calculated by MATLAB. Discrimination factor formula: $DF = ([F_{PM}] - \text{background})/([F_{MM}] - \text{background})$.

RESULTS AND DISCUSSION

Fault tolerance of Cas12a for an ss-activator

Studies have shown that single-base mismatches of ss-activators hardly affect the activation of Cas12a (6), but the fault tolerance of Cas12a for ss-activators has not been fully verified (the term 'fault' refers to any difference between the actual activator analog and the perfectly matched true activator, such as mismatch, bulge, split, gap, etc.). As shown in Supplementary Figures S1 and S9, types of faulty ss-activators were used to activate Cas12a, and the percentage of reporter cleaved represents the activation efficiency.

Downloaded from https://academic.oup.com/nar/advance-article/doi/10.1093/nar/gkac886/6786210 by Shanghai Normal University user on 03 November 2022

Cas12a can still be activated incorrectly when the number of mismatched bases at the 3′ end of the activator is within 6 nt (Supplementary Figure S1A), within 9 nt bases at the 5′ end (Supplementary Figure S1B), within 4 nt bases at both ends (Supplementary Figure S1C) and within 2 nt bases in the interior (Supplementary Figure S1D). The fault tolerance of Cas12a for ss-activator mismatch is interior < both ends < 3′ end < 5′ end. The insertions of bulge loops (BLs) within 3 nt in length internally, at the 3′ end and 5′ end of the ss-activator (Supplementary Figures S1E–G) all resulted in incorrect activation. The fault tolerance of Cas12a for the ss-activator's BL insertion is 3′ end < 5′ end < interior. With splitting of the activator in half down the middle and deleting bases within 2 nt (Supplementary Figure S1H) or extending base pairs within 9 nt (Supplementary Figure S1I), Cas12a remained incorrectly activated. The results showed that Cas12a was highly tolerant of all types of erroneous ss-activators.

It follows that this mode is not only useless in single-base mismatched recognition, but the ss-activator analogs produced by out-of-control amplifying or other side reactions may also interfere severely with Cas12a activation. Although the ss-activation mode does not require a PAM and allows free choice of activator sequences, it is highly fault tolerant. In other words, it is severely lacking in specificity and stability, and unsuitable for applications in high-precision molecular recognition.

Unrestricted novel CRISPR–Cas12a activation mode

In addition to ss-activators, Cas12a can be activated by ds-activators. The PAM of ds-activators can guide the Cas–crRNA complex to unravel the dsDNA from the seed region to form an R-loop and allosterically active Cas (29). Although the necessity for PAM recognition allows the ds-activation mode to have considerably less fault tolerance, it also severely constrains universality and flexibility of this mode.

Several studies have attempted to find more available PAM sequences, but they could not completely eliminate the sequence restrictions. Kleinstiver developed variants of the CRISPR enzyme to eliminate the PAM requirement, but not using the PAM can reduce the accuracy and cause off-targeting (30,31). In addition to studies targeting the Cas nuclease itself, several nucleic acid technologies have played a role. Jiang (21) inserted a PAM near the mutation site via PCR; Hsing (22) assembled ss-targets with probes containing a PAM; and Nie (29) introduced bubbles in ds-targets, skipping the PAM-guided strand unraveling step.

These studies have achieved good results, but still required the fine-tuning of the PAM or bubble insertion positions for different target sequences or optimization of probe and primer design and can hardly be applied to recognition of all target sequences. Therefore, a new activation mode with substantially superior specificity and universality is urgently needed for the further development of CRISPR technology.

Construction and working principle of TOA

Any ds-oligonucleotide containing a toehold rapidly undergoes TSDR with the corresponding ss-oligonucleotide, releasing the protected strand and forming a new ds-structure (23). The reaction is universal and programmable, which inspired us to design the TOA.

The TOA is a ds-DNA containing a toehold, and it can rapidly undergo TSDR with ss-crRNA (Schematic 1C), activating Cas12a without a PAM. As shown in Figure 1A, similar to conventional TSDR, a TOA with a toehold longer than 7 nt produces a high signal. However, the signal generated by a 1 nt toehold TOA is unexpectedly high, and signal leakage occurs with the use of a 0 nt TOA (cleaved reporter percentage >13%). This finding may be due to the strong binding affinity of the DNA–RNA complex and a certain effect of the Cas nuclease (32). Supplementary Figure S2 shows the relationship between the yield of conventional TSDR and toehold length. To further stabilize the reaction, we extended a segment of meaningless sequence (stabilizer) at the end of the TOA's short strand and observed that the signal leakage was significantly reduced (Figure 1B). This result may be due to the stabilized DNA duplex resulting from the increase in base stacking force and the decrease in DNA breathing (33). By combining the stabilizer with a toehold of different lengths, a more regular signal output was achieved, which was consistent with the conventional TSDR (Figure 1C). As shown in Figure 1D–F, a homologous conclusion can be obtained with the reversed direction and position of the toehold and stabilizer.

This method, which is far more universal than the ds-activation mode, totally eliminates the need for a PAM and achieves homologous results for different toehold orientations, positions and sequences. In addition, the strict regularity makes the TOA mode more stable than the highly fault-tolerant ss-activation mode. Moreover, TSDR is one of the important cornerstones of DNA dynamic nanotechnology, and the regularity highly similar to that of TSDR allows for the increased adjustability and programmability of this activation mode (23). The activation efficiency can be modulated by changing the length or structure [such as an allosteric toehold (34), remote toehold (35) and associative toehold (36)] of the toehold or taking advantage of its variable hybridization activity to make CRISPR technologically compatible with wide molecular reaction networks.

Identification of single-base mismatches in TOA

The velocity of TSDR is significantly reduced when single-base mismatches occur on or near the toehold (25,38) To investigate whether TOA has a similar specificity, we compared the effects of four single-base mutations at different positions (Mutation-1, Mutation-2, Mutation-3 and Mutation-4) on the signal generated by TOA (Supplementary Figure S3) and calculated the DFs (Figure 2).

As presented in Figure 2A, the TOA containing one toehold was named TOA-α, and the TOA containing a toehold and a stabilizer was named TOA-β. When the toehold was at the TOA's 5′ end (5′ TOA-α and 5′ TOA-β), Mutation-4 was on the toehold, Mutation-3 was near the toehold, Mutation-2 was in the middle of the TOA and Mutation-1 was at the far end of the TOA. When the position of the toehold was reversed (3′ TOA-α and 3′ TOA-β), the positional relationships of the four mutations also become reversed. When the TOA-α's toehold length was 5 nt (Fig-

Downloaded from https://academic.oup.com/nar/advance-article/doi/10.1093/nar/gkac886/6786210 by Shanghai Normal University user on 03 November 2022

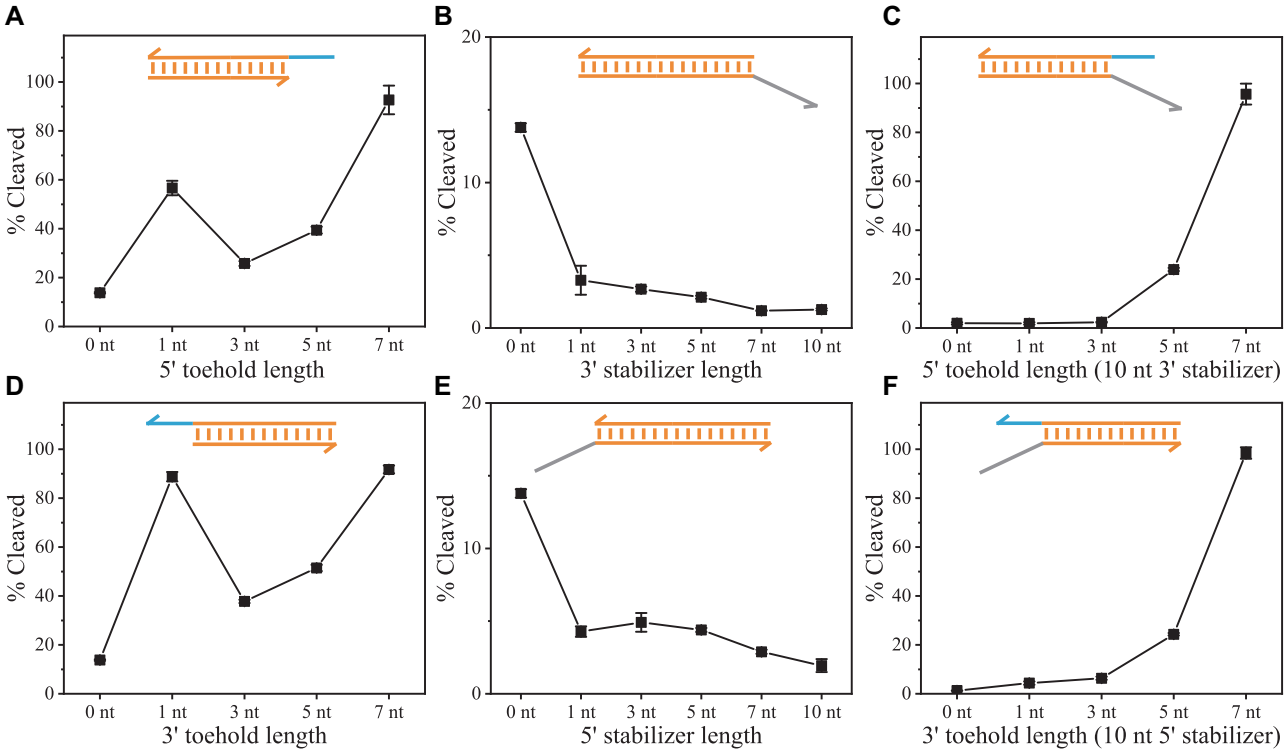


Figure 1. The construction and performance of a TOA. Blue represents the toehold; gray represents the stabilizer. The activity of Cas12a trans-cleavage activated by TOAs containing different lengths of 5′ toehold (**A**) and 3′ toehold (**D**), and that by a toehold-less TOA containing different lengths of 3′ stabilizer (**B**) and 5′ stabilizer (**E**). The activity of Cas12a trans-cleavage activated by TOA containing a 10 nt 3′ stabilizer and different lengths of 5′ toehold (**C**), and that by a 10 nt 5′ stabilizer and different lengths of 3′ toehold (**F**). Error bars represented the standard deviation calculated from three independent experiments.

ure 2B) and 7 nt (Figure 2C), the DFs of mutations near the toehold were higher, and were significantly higher than those on the ss-activator, respectively. Although the signal intensity generated by a 7 nt toehold TOA-α (Supplementary Figure S3C, D) was considerably stronger than that of the 5 nt toehold TOA-α (Supplementary Figure S3A, B), the discriminatory capacity was not evidently improved, which may be due to the shorter ds-domain and less stable structure of the 7 nt toehold TOA. As shown in Figure 2D, TOA-β (Supplementary Figure S3E, F) with a 7 nt toehold exhibited higher specificity than TOA-α, and its DF at Mutation-1 was ∼40-fold higher than that of the ss-activator. Although the specificity of the ds-activator (with a PAM) was better than that of the ss-activator (DF 2.8: 1.1 for Mutation-1 near a PAM), it was still substantially less than that of TOA-β (DF 2.8: 40.0) (Supplementary Figure S4A–C). We repeated this experiment with different sequences (both activation sequences and stabilizer sequences) and still obtained the same conclusion (Supplementary Figures S5 and S6). Characterization of TOA-β specificity by polyacrylamide gel electrophoresis (PAGE) is given in Supplementary Figure S7.

Thus, TOA-β possesses a significantly higher specificity than ds- and ss-activators, and the specificity for different mutations is highly correlated with the toehold, which indicates that we can flexibly modulate the detection performance by changing the length and position of the toehold. Different from adjusting the insertion position of a PAM or bubble, a distinctive toehold can be easily obtained for any dsDNA. Therefore, this mode of activation reduces the risk of insertion errors or failures, and has almost no sequence restriction, so that it can be extended to any target.

Combination of BM reaction and TOA

The BM is a reversible reaction without base pair changes ($\Delta G \approx 0$) (29). Thus, a single-base mismatch, which causes minute thermodynamic changes, can break the equilibrium and significantly reduce the reaction yield ($\Delta G > 0$). The relationship between the ΔG and yield was shown in Supplementary Figure S8. Although the specificity of the BM reaction is high, the yield is only ∼0.5 due to its reversible feature. Structurally, TOA-β is similar to a reacted BMP, which both contain a ds-domain, a toehold and a stabilizer (Supplementary Scheme S13). Theoretically, the reversible BM reaction and irreversible TSDR combination can improve the reaction yield and, with addition of the signal amplification of Cas12a, the detection performance can be further improved (called the BM-TOA system).

As shown in Figure 3A, after binding to the ss-domain of the BMP (gray part), only the perfectly matched ss-target can trigger the BM, releasing a short ss-sequence as a toehold (blue part) of TOA and undergoing TSDR with the crRNA. Ultimately, the activated Cas12a amplified the fluorescent signal (the activator is ss- or ds-oligonucleotide with the ability to activate Cas nuclease, which is distinct from an input target nucleic acid). As shown in Figure 3B and C, the BM domain of BMP (i.e. TOA's toehold) can produce a

Downloaded from https://academic.oup.com/nar/advance-article/doi/10.1093/nar/gkac886/6786210 by Shanghai Normal University user on 03 November 2022

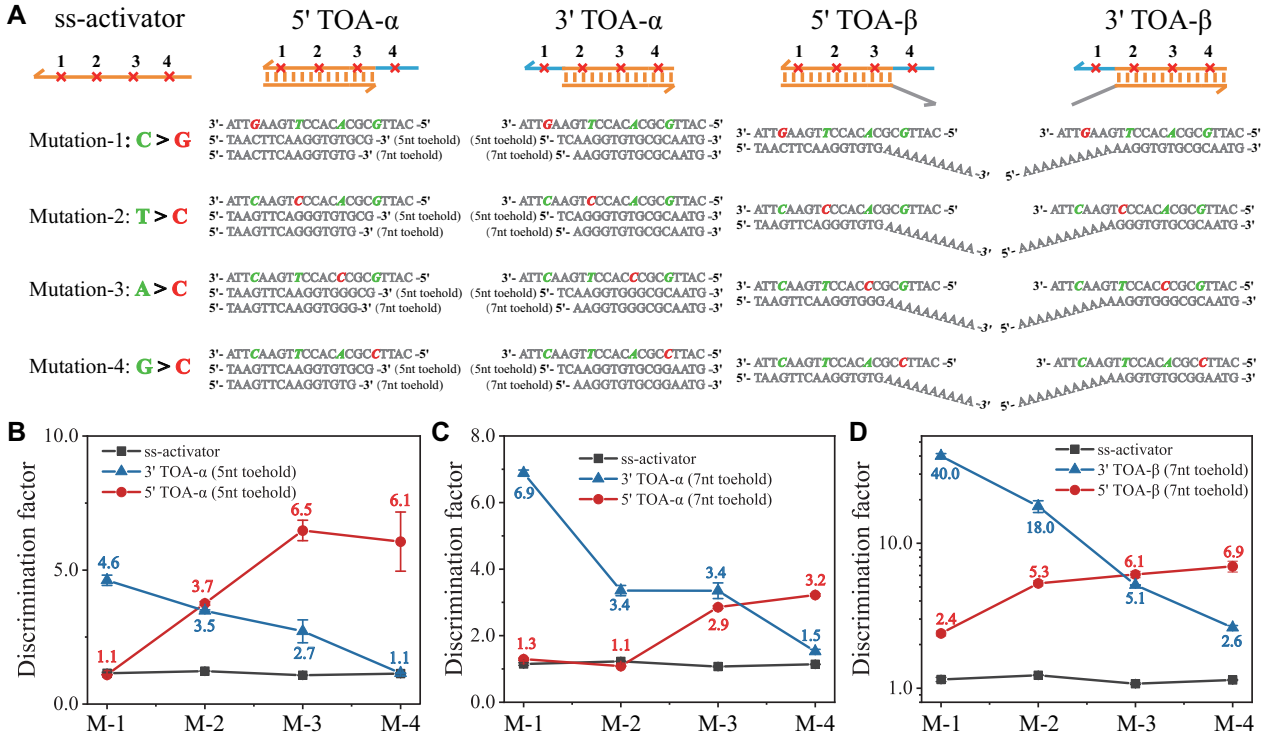


Figure 2. Specificity of activators containing different point mutations at different position. (**A**) Scheme diagram of different activators and different mutations. Green letters represent wild-type bases, red letters represent mutant-type bases and red '×' represents mutation positions. (**B**) The DFs of 5′ TOA-α and 3′ TOA-α (5 nt toehold). (**C**) The DFs of 5′ TOA-α and 3′ TOA-α (7 nt toehold). (**D**) The DFs of 5′ TOA-β and 3′ TOA-β (7 nt toehold). Error bars represented the standard deviation calculated from three independent experiments.

high signal at longer than 6 nt and has the highest DF (88.7) at 7 nt, which was considerably higher than that of TOA-β alone (6.9). Figure 3D and E further demonstrates that the high discrimination effect was a joint effect of the BM reaction and the TOA-mediated CRISPR system. For perfectly matched targets, the reporter-cleaved percentage of the BM-TOA system reached 81% in 24 min; for mismatched targets, the DFs were 88.7 (G > C), 35.1 (G > A) and 82.7 (G > T) (Figure 3D). However, excluding the CRISPR system (replacing Cas12a and Cas-reporter with the TSDR-reporter), the reporter-reacted percentage was only 1%, and the DFs were only 5.7, 4.6 and 5.6, respectively (Figure 3E). This result indicates that the BM-TOA system integrated both the high specificity of the BM reaction and TSDR and the sensitivity of the CRISPR system. Finally, we detected all mismatch types using the BM-TOA system. All results showed extremely high specificity (Figure 3F; Supplementary Figure S9), including T:G and G:T mismatches, the most difficult type (Supplementary Table S2). Characterization of BM-TOA specificity by PAGE is shown in Supplementary Figure S10.

The BM-TOA system possesses excellent single-base mismatch specificity without introducing any additional mismatches in crRNA (21,32,37,38) and can be widely used as a high-performance CRISPR–Cas12a platform for detection of various types of mutations. In addition, the system also proved the compatibility of the TOA activation mode: the TOA has the potential to cascade with various reaction networks.

Low-abundance point mutation detection

Although it is difficult for mismatched ss-targets to trigger the BM reaction, they still can bind to the ss-domain of BMPs. Therefore, when the mutation abundance is low, the probe will be massively consumed and wasted by wild-type targets. As is shown in Supplementary Figure S11, for ss-targets, BMP hardly distinguished a 5% mutation. We presumed that the problem could be solved by using ss-probes (triggers) to detect BMP-like targets. The complementary domain between the trigger and crRNA was only 7 nt, which hardly results in signal leakage. Thus, excess triggers can be added to increase the binding probability of mutant-type targets without any risk (Supplementary Figure S12). Moreover, amplifying BMP-like targets may be more stable, because their main structure is double-stranded, with less self-hybridization (23,39).

As shown in Figure 4A, we designed two methods to obtain BMP-like targets: U-PCR and C3-PCR. In U-PCR, the T-bases in the U-forward primers were replaced with U-bases (deoxyuridine nucleotides), and the ss-domain is exposed by digestion of the U-bases using UDG after amplification. In C3-PCR, an extra ss-domain (green part) is added to the 5′ end of the forward primer, separated by a C3 spacer. The strand extension of the ss-domain can be blocked by the C3 spacer, so the products directly contain the ss-domain. After BMP-like targets were obtained, saturating triggers are used to bind with them, and only the matched partners will undergo the BM reaction and release the toeholds of BMP-like targets. Different from ss-target detection, the re-

Downloaded from https://academic.oup.com/nar/advance-article/doi/10.1093/nar/gkac886/6786210 by Shanghai Normal University user on 03 November 2022

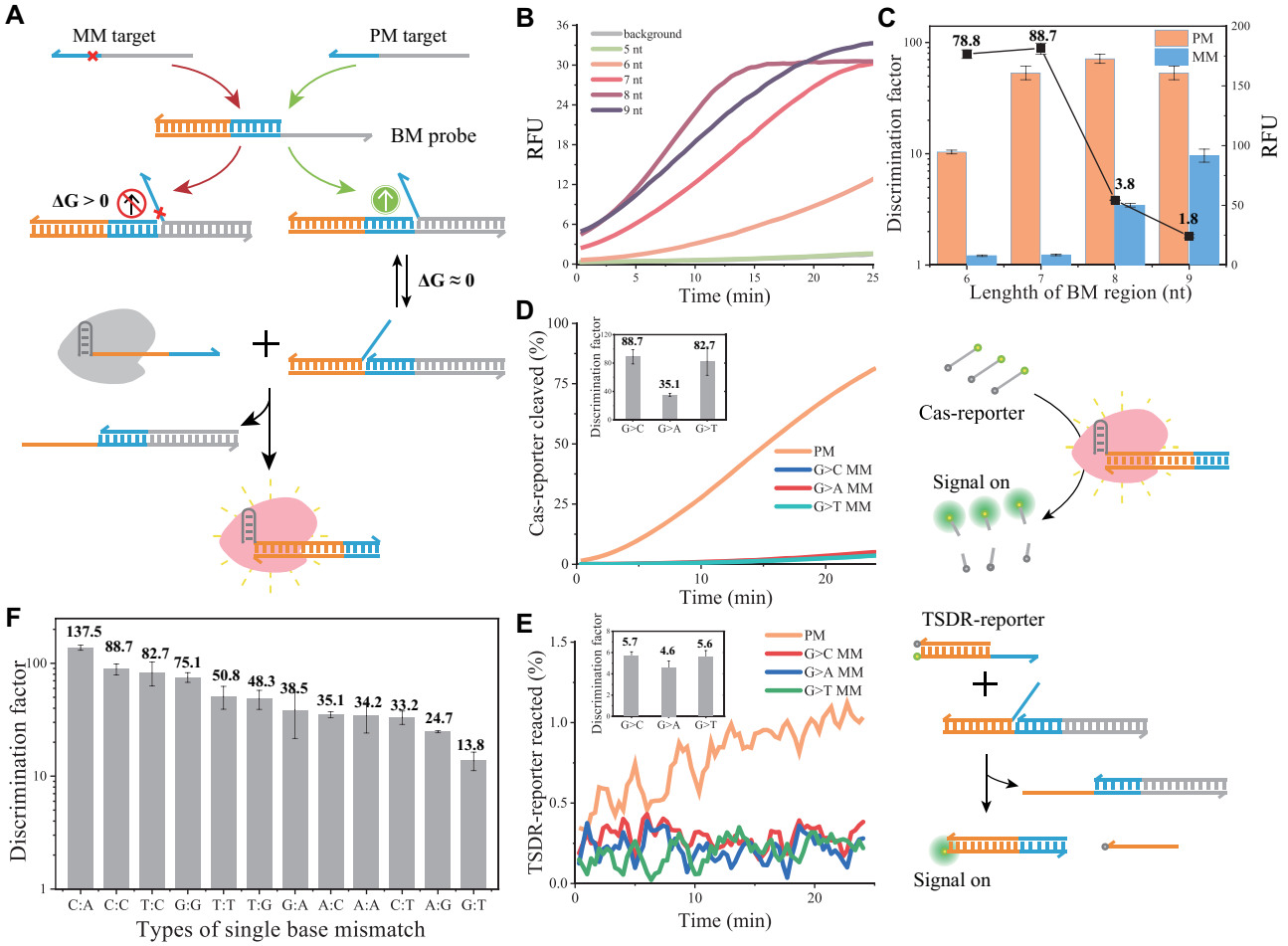


Figure 3. The performance of BM-TOA. (**A**) Working principle of the BM-TOA system. (**B**) Fluorescence kinetic curves generated by the BM-TOA system with different lengths of branching migration domains. (**C**) DFs of BM-TOA systems with different length branching migration domains for G > C mutations. The BM-TOA system with (**D**) and without (**E**) the CRISPR system detected fluorescence kinetic curves and DFs for different mismatches. (**F**) The DFs of all types of single-base mismatches by the BM-TOA system.

leased toeholds are from the BMP-like targets themself, not from the synthetic BMP. Thus, the mutation information is retained in the toeholds and will be subject to the second identification by TSDR. It is reasonable to speculate that this may lead to higher detection accuracy. The data from Figure 4B and C demonstrated that the specificity of the BMP-like target was higher than that of the ss-target in both systems. Also, in the C3-PCR system, we detected 0.5% mutation in BMP-like targets (Supplementary Figure S13), and in the U-PCR system we detected 0.05% (Supplementary Figure S14). T790M mutation and L858R mutation in the EGFR gene are closely related to the diagnosis and prognosis of non-small cell lung cancer and detecting them is of great clinical value. As shown in Figure 4D–G, the BM-TOA system detected 0.1% T790M mutation and L858R mutation, and the mutation abundance was linearly correlated with fluorescence.

In Figure 3C, the DF is significantly reduced when the length of the BM domain was increased to 9 nt, but in Figure 4A, the length of the BM domain in the C3-PCR system is much longer than that of U-PCR, the specificities were also satisfying. This is because the toehold domain and the BM domain of the U-PCR system are equal, although having a longer BM domain, the length of the toehold domains (blue marked) in the C3-PCR system and U-PCR both are 7 nt. It can be seen that the toehold length is the most important factor in determining specificity.

Practical application

U-PCR showed a superior performance (Supplementary Figure S14) and was applied for the subsequent assays. As shown in Supplementary Figure S15, the melting peak of the amplification products with the U-forward primer was 82°C, and it decreased to 76°C after UDG treatment. The melting peak is shifted to the left, indicating that UDG digested the U-base of the products, reduced the number of base pairs and exposed the ss-domain. Supplementary Figure S16 shows the characterization results of PAGE. Subsequently, we amplified the L858R (Supplementary Figure S17) and T790M (Supplementary Figure S18) mutations at different abundances of 1 fmol by U-PCR and detected them with the BM-TOA system, which was able to detect

Downloaded from https://academic.oup.com/nar/advance-article/doi/10.1093/nar/gkac886/6786210 by Shanghai Normal University user on 03 November 2022

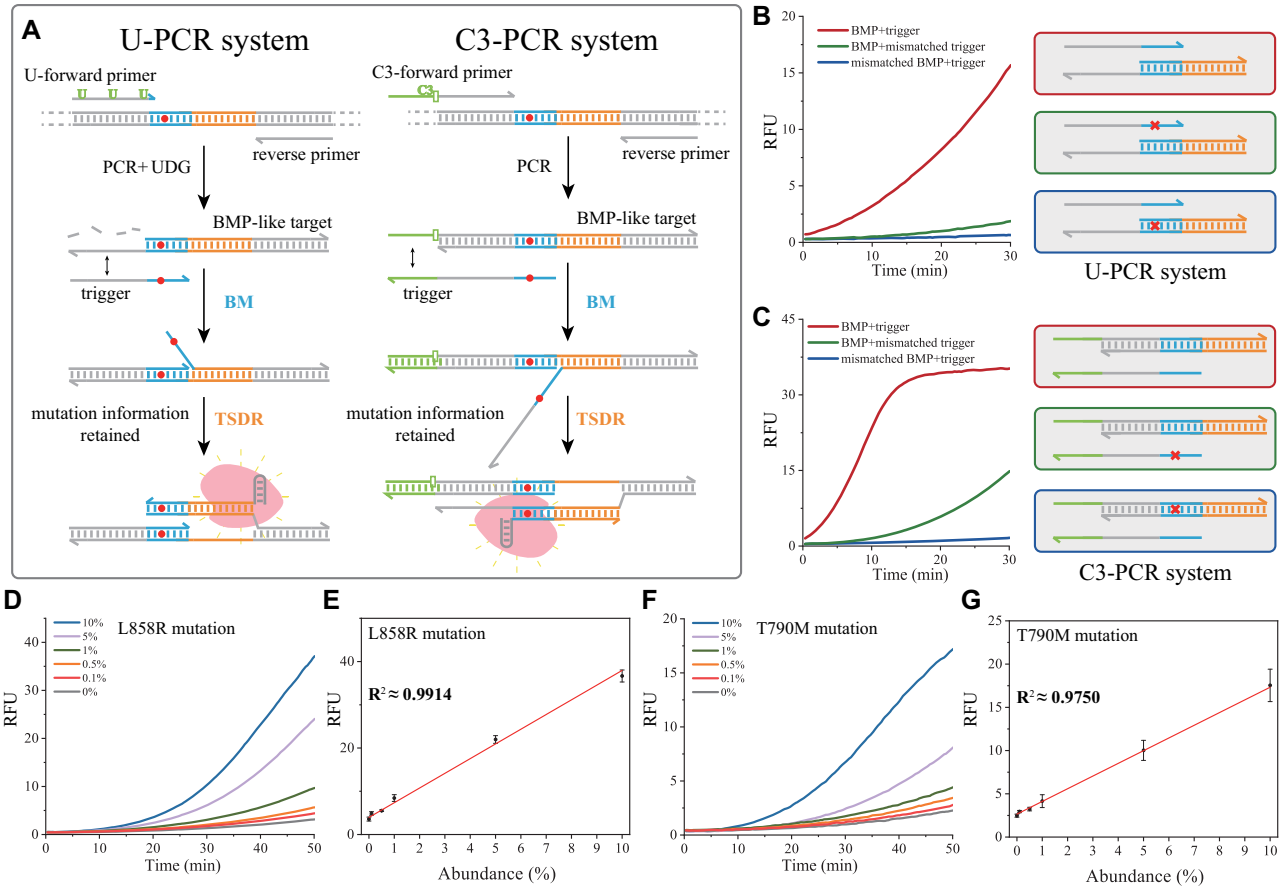


Figure 4. Detection of low-abundance point mutations in BMP-like targets by ss-trigger probes. (**A**) Schematic diagram of two improved PCR to acquire BMP-like targets and detect them by the BM-TOA system. The red circle represents mutation sites to be detected. The green 'U' and 'C3' represent deoxyuracil nucleotide and C3 spacer modification sites, respectively. Comparison of the specificity for detecting ss-targets and BMP-like targets in the U-PCR (**B**) and C3-PCR (**C**) system. The red '×' represents mismatch sites. Fluorescence kinetic curves (**D**, L858R; **F**, T790M) and linear fitting (**E**, L858R; **G**, T790M) for the detection of mutations of different abundance are shown.

mutations down to 0.05%. L858R is one of the most difficult point mutations to detect due to the high GC content surrounding it (GGGCTGGCC > GGGCGGGCC) and the small ΔG it caused. As is shown in Supplementary Figure S19, we take this mutation as the target to test the ability of the BM-TOA system in discriminating mutation in clinical samples, and the results by the BM-TOA system were very consistent with those by dPCR (Supplementary Tables S3 and S4).

In most post-PCR assays, ss-targets with hybridization activity are amplified to trigger the subsequent detection step, but it needs to unravel the potential self-hybridization of the targets by raising the reaction temperature (23,38). Fortunately, the main structure of the BMP-like target is a stable double strand almost without a troublesome secondary structure. In addition, excess reverse primers could generate abundant complementary sequences that sufficiently bind potential ss-activator analogs and eliminate their interference, so amplification products can be detected without purification. Thus, the BM-TOA system is specific, sensitive, stable and universal, and may show great potential in basic research and clinical diagnosis related to tumors and genetic diseases.

CONCLUSION

In summary, we proposed a simple but powerful CRISPR–Cas12a activation mode based on TSDR and BM. The TOA was confirmed to be a powerful activator by systematically studying its working principles and performance. In combination with BM, the BM-TOA system achieved more specific and universal identification of all mismatch types without introducing any additional mismatches in crRNA. The concordance between the detection results of clinical samples with L858R mutations and the dPCR results further demonstrated its practical application potential.

This approach has several advantages over ss- or ds-activation modes. Firstly, the toehold of TOA is conditionally released by BM reaction and then binds to crRNA by strict TSDR, which greatly improves the activation specificity of Cas12a. Secondly, the cascade of TSDR and BM allows us to regulate the reaction in a simple and flexible manner to achieve controlled activation without the signal leakage caused by invasion strands. Moreover, unlike the insertion of a PAM or bubble by changing sequence, a distinctive toehold can be easily obtained for any dsDNA. Thus, this activation mode not only avoids the risk of insertion errors or failures but is also not limited by the sequence environ-

Downloaded from https://academic.oup.com/nar/advance-article/doi/10.1093/nar/gkac886/6786210 by Shanghai Normal University user on 03 November 2022

ment of the target, greatly broadening the choice of available activator sequences. The combination with dynamic DNA nanotechnology also allows for a high degree of sequence programmability. The accurate activation of different targets can be achieved by a simple change in the toehold position. Changing the toehold length can adjust the activation efficiency, and a toehold with variable hybridization activities can serve as a reusable interface, which allows the TOA to be compatible with a wider molecular reaction network. Most importantly, although our work is based on Cas12a, this activation mode has no strict requirement for Cas nuclease subtypes and is potentially scalable to other CRISPR–Cas systems. These advantages of the BM-TOA strategy allow CRISPR technology to play a greater and more important role not only in biomedical but also in high-precision molecular sensing, biochemical circuits, molecular reaction networks, etc.

In this work, we assay the actual sample still requiring sample amplification and processing by PCR, which can be a cumbersome process. However, with the development of isothermal amplification techniques and microfluidics, this will not be a problem worth bothering about. There has been much work combining techniques such as Recombinase Polymerase Amplification (RPA) (7), Rolling Circle Amplification (RCA) (40) and Primer Exchange Reaction (PER) (41) with CRISPR technology, and it has even been demonstrated that they can be combined in a single step (15). This integration may make the BM-TOA technique an even more promising tool for point-of-care testing.

DATA AVAILABILITY

All data supporting the findings of this study are available within the article and its supplementary information or will be made available from the authors upon request.

SUPPLEMENTARY DATA

Supplementary Data are available at NAR Online.

FUNDING

This research work was financially supported by the National Natural Science Foundation of China [82172369 and 81972025]; the Natural Science Foundation of Chongqing, China [cstc2021jcyj-msxmX0326]; and the Chongqing Postgraduate Research Innovation Project [CYB22219].
Conflict of interest statement. None declared.

REFERENCES

1. Knott,G.J. and Doudna,J.A. (2018) CRISPR-Cas guides the future of genetic engineering. *Science*, **361**, 866–869.
2. Shi,K., Xie,S., Tian,R., Wang,S., Lu,Q., Gao,D., Lei,C., Zhu,H. and Nie,Z. (2021) A CRISPR-Cas autocatalysis-driven feedback amplification network for supersensitive DNA diagnostics. *Sci. Adv.*, **7**, eabc7802.
3. Dai,Y., Wu,Y., Liu,G. and Gooding,J.J. (2020) CRISPR mediated biosensing toward understanding cellular biology and point-of-care diagnosis. *Angew. Chem. Int. Ed.*, **59**, 20754–20766.
4. Wei,Y., Yang,Z., Zong,C., Wang,B., Ge,X., Tan,X., Liu,X., Tao,Z., Wang,P., Ma,C. *et al.* (2021) Trans single-stranded DNA cleavage via CRISPR/Cas14a1 activated by target RNA without destruction. *Angew. Chem. Int. Ed.*, **60**, 24241–24247.
5. Kaminski,M.M., Abudayyeh,O.O., Gootenberg,J.S., Zhang,F. and Collins,J.J. (2021) CRISPR-based diagnostics. *Nat. Biomed. Eng.*, **5**, 643–656.
6. Chen,J.S., Ma,E., Harrington,L.B., Da Costa,M., Tian,X., Palefsky,J.M. and Doudna,J.A. (2018) CRISPR-Cas12a target binding unleashes indiscriminate single-stranded DNase activity. *Science*, **360**, 436–439.
7. Gootenberg,J.S., Abudayyeh,O.O., Kellner,M.J., Joung,J., Collins,J.J. and Zhang,F. (2018) Multiplexed and portable nucleic acid detection platform with cas13, cas12a, and csm6. *Science*, **360**, 439–444.
8. Tang,Y., Gao,L., Feng,W., Guo,C., Yang,Q., Li,F. and Le,X.C. (2021) The CRISPR–Cas toolbox for analytical and diagnostic assay development. *Chem. Soc. Rev.*, **50**, 11844–11869.
9. Tang,Y., Qi,L., Liu,Y., Guo,L., Zhao,R., Yang,M., Du,Y. and Li,B. (2022) CLIPON: a CRISPR-enabled strategy that turns commercial pregnancy test strips into general point-of-need test devices. *Angew. Chem. Int. Ed.*, **61**, 202115907.
10. Bruch,R., Baaske,J., Chatelle,C., Meirich,M., Madlener,S., Weber,W., Dincer,C. and Urban,G.A. (2019) CRISPR/Cas13a-powered electrochemical microfluidic biosensor for nucleic acid amplification-free miRNA diagnostics. *Adv. Mater.*, **31**, 1905311.
11. Lièvre,A., Bachet,J.-B., Le Corre,D., Boige,V., Landi,B., Emile,J.-F., Côté,J.-F., Tomasic,G., Penna,C., Ducreux,M. *et al.* (2006) KRAS mutation status is predictive of response to cetuximab therapy in colorectal cancer. *Cancer Res.*,**66**, 3992–3995.
12. Bronner,C.E., Baker,S.M., Morrison,P.T., Warren,G., Smith,L.G., Lescoe,M.K., Kane,M., Earabino,C., Lipford,J., Lindblom,A. *et al.* (1994) Mutation in the DNA mismatch repair gene homologue hMLH 1 is associated with hereditary non-polyposis colon cancer. *Nature*, **368**, 258–261.
13. Shah,S.P., Morin,R.D., Khattra,J., Prentice,L., Pugh,T., Burleigh,A., Delaney,A., Gelmon,K., Guliany,R., Senz,J. *et al.* (2009) Mutational evolution in a lobular breast tumour profiled at single nucleotide resolution. *Nature*, **461**, 809–813.
14. Rabinowitz,R., Almog,S., Darnell,R. and Offen,D. (2020) CrisPam: SNP-derived PAM analysis tool for allele-specific targeting of genetic variants using CRISPR-Cas systems. *Front. Genet.*, **11**, 851.
15. Ding,X., Yin,K., Li,Z., Lalla,R.V., Ballesteros,E., Sfeir,M.M. and Liu,C. (2020) Ultrasensitive and visual detection of SARS-CoV-2 using all-in-one dual CRISPR-Cas12a assay. *Nat. Commun*, **11**, 4711.
16. Zetsche,B., Gootenberg,J.S., Abudayyeh,O.O., Slaymaker,I.M., Makarova,K.S., Essletzbichler,P., Volz,S.E., Joung,J., van der Oost,J., Regev,A. *et al.* (2015) Cpf1 is a single RNA-guided endonuclease of a class 2 CRISPR-Cas system. *Cell*, **163**, 759–771.
17. Jeon,Y., Choi,Y.H., Jang,Y., Yu,J., Goo,J., Lee,G., Jeong,Y.K., Lee,S.H., Kim,I.-S., Kim,J.-S. *et al.* (2018) Direct observation of DNA target searching and cleavage by CRISPR-Cas12a. *Nat. Commun*, **9**, 2777.
18. Teng,F., Guo,L., Cui,T., Wang,X.-G., Xu,K., Gao,Q., Zhou,Q. and Li,W. (2019) CDetection: CRISPR-Cas12b-based DNA detection with sub-attomolar sensitivity and single-base specificity. *Genome Biol.*, **20**, 132.
19. Li,S.-Y., Cheng,Q.-X., Wang,J.-M., Li,X.-Y., Zhang,Z.-L., Gao,S., Cao,R.-B., Zhao,G.-P. and Wang,J. (2018) CRISPR-Cas12a-assisted nucleic acid detection. *Cell Discov*, **4**, 20.
20. Guo,L., Sun,X., Wang,X., Liang,C., Jiang,H., Gao,Q., Dai,M., Qu,B., Fang,S., Mao,Y. *et al.* (2020) SARS-CoV-2 detection with CRISPR diagnostics. *Cell Discov*, **6**, 34.
21. Chen,Y., Mei,Y. and Jiang,X. (2021) Universal and high-fidelity DNA single nucleotide polymorphism detection based on a CRISPR/Cas12a biochip. *Chem. Sci.*, **12**, 4455–4462.
22. Lee Yu,H., Cao,Y., Lu,X. and Hsing,I.-M. (2021) Detection of rare variant alleles using the ascas12a double-stranded DNA trans-cleavage activity. *Biosens. Bioelectron.*, **189**, 113382.
23. Khodakov,D.A., Khodakova,A.S., Linacre,A. and Ellis,A.V. (2013) Toehold-mediated nonenzymatic DNA strand displacement as a platform for DNA genotyping. *J. Am. Chem. Soc.*, **135**, 5612–5619.
24. Tang,W., Zhong,W., Tan,Y., Wang,G.A., Li,F. and Liu,Y. (2020) DNA strand displacement reaction: a powerful tool for discriminating single nucleotide variants. *Top. Curr. Chem. (Cham)*, **378**, 10.
25. Li,X., Zhang,D., Gan,X., Liu,P., Zheng,Q., Yang,T., Tian,G., Ding,S. and Yan,Y. (2021) A cascade signal amplification based on dynamic

Downloaded from https://academic.oup.com/nar/advance-article/doi/10.1093/nar/gkac886/6786210 by Shanghai Normal University user on 03 November 2022

DNA nanodevices and CRISPR/Cas12a trans-cleavage for highly sensitive microRNA sensing. *ACS Synth. Biol.*, **10**, 1481–1489.
26. Wang,C., Han,C., Du,X. and Guo,W. (2021) Versatile CRISPR-Cas12a-based biosensing platform modulated with programmable entropy-driven dynamic DNA networks. *Anal. Chem.*, **93**, 12881–12888.
27. Xiong,Y., Zhang,J., Yang,Z., Mou,Q., Ma,Y., Xiong,Y. and Lu,Y. (2020) Functional DNA regulated CRISPR-Cas12a sensors for point-of-care diagnostics of non-nucleic-acid targets. *J. Am. Chem. Soc.*, **142**, 207–213.
28. Xiao,X., Wu,T., Xu,L., Chen,W. and Zhao,M. (2017) A branch-migration based fluorescent probe for straightforward, sensitive and specific discrimination of DNA mutations. *Nucleic Acids Res.,***45**, e90.
29. Chen,S., Wang,R., Peng,S., Xie,S., Lei,C., Huang,Y. and Nie,Z. (2022) PAM-less conditional DNA substrates leverage trans-cleavage of CRISPR-Cas12a for versatile live-cell biosensing. *Chem. Sci.*, **13**, 2011–2020.
30. Rosello,M., Serafini,M., Mignani,L., Finazzi,D., Giovannangeli,C., Mione,M.C., Concordet,J.-P. and Del Bene,F. (2022) Disease modeling by efficient genome editing using a near PAM-less base editor in vivo. *Nat. Commun*, **13**, 3435.
31. Collias,D. and Beisel,C.L. (2021) CRISPR technologies and the search for the PAM-free nuclease. *Nat. Commun*, **12**, 555.
32. Kim,H., Lee,W., Oh,Y., Kang,S.-H., Hur,J.K., Lee,H., Song,W., Lim,K.-S., Park,Y.-H., Song,B.-S. *et al.* (2020) Enhancement of target specificity of CRISPR–Cas12a by using a chimeric DNA–RNA guide. *Nucleic Acids Res.*, **48**, 8601–8616.
33. Srinivas,N., Ouldridge,T.E., Šulc,P., Schaeffer,J.M., Yurke,B., Louis,A.A., Doye,J.P.K. and Winfree,E. (2013) On the biophysics and kinetics of toehold-mediated DNA strand displacement. *Nucleic Acids Res.,***41**, 10641–10658.
34. Yang,X., Tang,Y., Traynor,S.M. and Li,F. (2016) Regulation of DNA strand displacement using an allosteric DNA toehold. *J. Am. Chem. Soc.*, **138**, 14076–14082.
35. Genot,A.J., Zhang,D.Y., Bath,J. and Turberfield,A.J. (2011) Remote toehold: a mechanism for flexible control of DNA hybridization kinetics. *J. Am. Chem. Soc.*, **133**, 2177–2182.
36. Chen,X. (2012) Expanding the rule set of DNA circuitry with associative toehold activation. *J. Am. Chem. Soc.*, **134**, 263–271.
37. Ke,Y., Huang,S., Ghalandari,B., Li,S., Warden,A.R., Dang,J., Kang,L., Zhang,Y., Wang,Y., Sun,Y. *et al.* (2021) Hairpin-spacer crRNA-enhanced CRISPR/Cas13a system promotes the specificity of single nucleotide polymorphism (SNP) identification. *Adv. Sci.*, **8**, 2003611.
38. Economos,N.G., Quijano,E., Carufe,K.E.W., Perera,J.D.R. and Glazer,P.M. (2022) Antispacer peptide nucleic acids for sequence-specific CRISPR-Cas9 modulation. *Nucleic Acids Res.,***50**, e59.
39. Luo,W., Wang,T., Weng,Z., Bai,S., Zhang,L., Wu,Y., Yu,H., Bai,D., Wang,D., Chen,H. *et al.* (2022) Bulge-loop tuned entropy-driven catalytic reaction and tag-encoded barcodes for multiplexed mutation detection, *Sens. Actuators B Chem.*, **358**, 131462.
40. Tian,B., Minero,G.A.S., Fock,J., Dufva,M. and Hansen,M.F. (2020) CRISPR-Cas12a based internal negative control for nonspecific products of exponential rolling circle amplification. *Nucleic Acids Res.*, **48**, e30.
41. Dai,Y., Xu,W., Somoza,R.A., Welter,J.F., Caplan,A.I. and Liu,C.C. (2020) An integrated multi-function heterogeneous biochemical circuit for high-resolution electrochemistry-based genetic analysis. *Angew. Chem. Int. Ed.*, **132**, 20726–20732.

Downloaded from https://academic.oup.com/nar/advance-article/doi/10.1093/nar/gkac886/6786210 by Shanghai Normal University user on 03 November 2022